Supplementary Information

Unveiling Transient Current Response in Bilayer Oxide-based Physical Reservoirs for Time-Series Data Analysis

Bo-Ru Lai [a], Kuan-Ting Chen [a], Rajneesh Chaurasiya[a,b], Song-Xian You [a], Wen-Dung Hsu [a], Jen-Sue Chen[a,c]*

[a] Department of Materials Science and Engineering, National Cheng Kung University, Tainan 70101, Taiwan

[b] Department of Electronics and Communication Engineering, Amrita School of Engineering, Amrita Vishwa Vidyapeetham, Chennai, India

[c] Academy of Innovative Semiconductor and Sustainable Manufacturing, National Cheng Kung University, Tainan 70101, Taiwan

**E-mail: jenschen@ncku.edu.tw*

Table S1. The comparison of electrical performances in different memristive devices.

Material	On/Off	Rectification ratio	Pulse condition	Ref.
Ta/IGZO/TaO_x/Pt	10^8	10^6	3 V/1 ms	This work
ITO/TiN/SiO_2/Si	10^4	-	3 V/250 µs	1
TiN/ZnO/NiO/Pt	~10^5	18.4	-4.5 V/10 ms	2
Al/TiN/HAO/n^{++}Si	>10^8	10^3	9.5 V/0.52 ms	3
W/TiN/SiO_2/Si	10^3	10	3.5 V/300 µs	4
Pd/Au/WO_x/W	-	3	1.5 V/1 ms	5
Ti/TaOx/TaOy/Pt	10^7	10^3	3 V/1 ms	6
Ag/mSiO2/TiN	10^7	-	3 V/100 µs	7

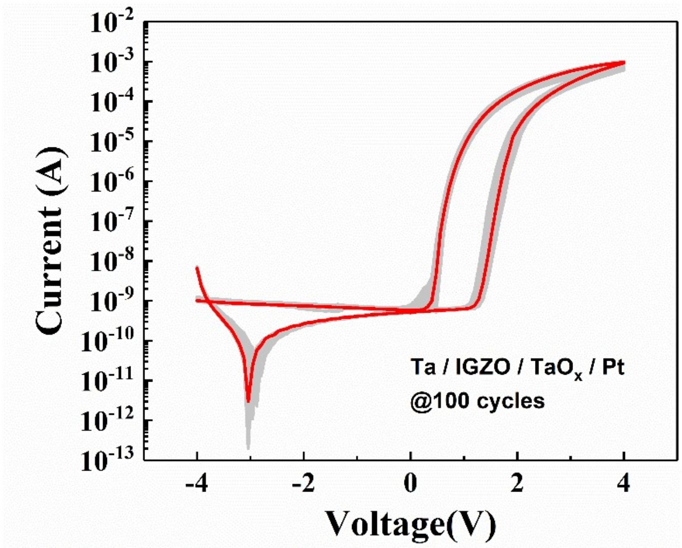

Figure S1. Consecutive I–V switching curves (100 times) for $|V_s|$ = 4 V of the device showing small variation during the cycles, indicating the stability and reliability of the device. Throughout the electrical measurements, the TE was maintained at ground potential, while the voltage was applied to the BE.

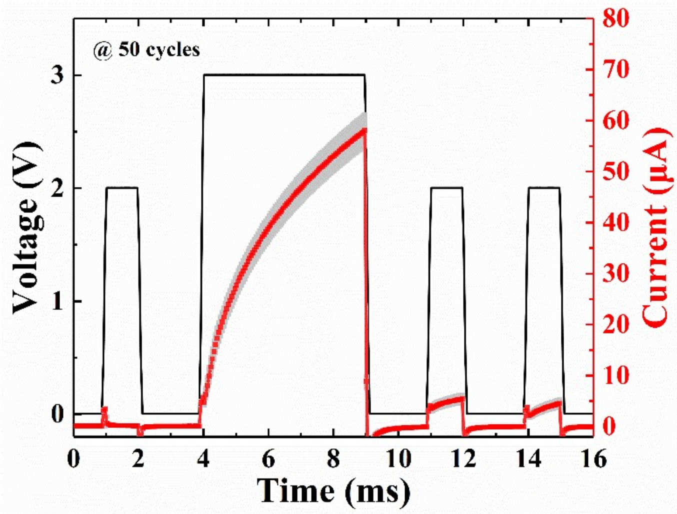

Figure S2. Prior to turning on the Ta/IGZO/TaO_x/Pt device, no current response was detected when applying small pulses of 2 V. However, once the device was stimulated by a large pulse of 5 V, a discernible current response was observed during subsequent small pulses. This consistent behavior was observed in 50 times, indicating the stability and uniformity of the current response over time.

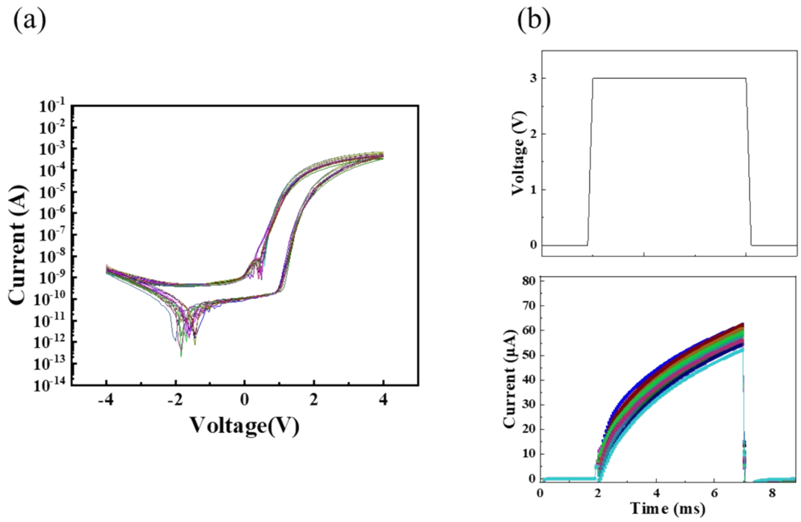

Figure S3. 16 memristive devices for (a) I-V measurement and (b) single pulse-triggered current responses.

The current-voltage (I-V) curves collected from 16 Ta/IGZO/TaOx/Pt dynamic memristive devices are shown in Figure S3(a), where the average current at the upper limit voltage (4 V) is 472 μA and the standard deviation is 80 μA, yielding a device-to-device variation of 0.17.

To verity the reliability of electrical pulse operation, a single pulse stimulation is applied on each memristor and the current response is recorded, as shown in Figure S3(b). The average maximum current value is 57 μA and standard deviation is 1.8 μA, yielding a device-to-device variation of 0.03.

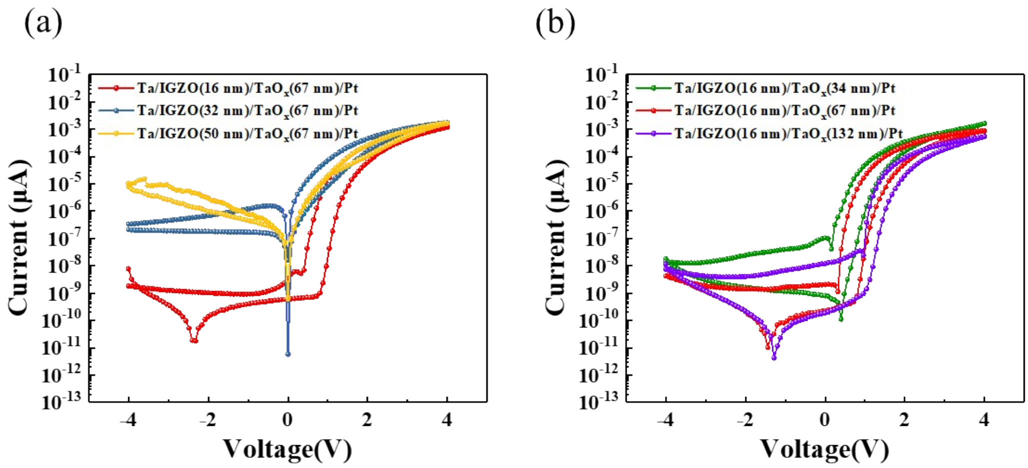

Figure S4. The I-V curves of Ta/IGZO/TaO_x/Pt device for changing the thicknesses of IGZO and TaO_x layers.

The standard device parameter in our work is Ta/IGZO (16 nm)/TaO_x (67nm)/Pt memristor. We have varied the thicknesses of both IGZO and TaO_x layer. First, the thickness of IGZO was increased from 16 nm to 32 and 50 nm. As revealed shown in Figure Rx(a), the currents at both positive and negative voltage shift to higher values, which makes the rectification ratio lower. In addition, the inexplicit current hysteresis loop of the 50 nm-IGZO device implies insignificant resistive switching behavior. For the TaO_x layer, as the thickness increases to 132 nm, the I-V curve shifts right and implies the voltage required to switch on the device is elevated. On the other hand, the On/Off and rectification ratio shrink as the TaO_x thickness decreases. Accordingly, we select the optimal thickness of 16 nm-IGZO and 67-nm TaO_x as our memristive device parameters.

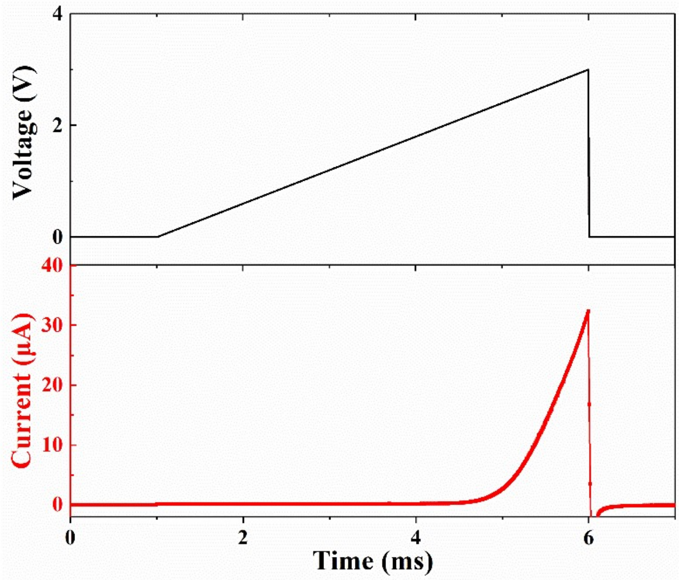

Figure S5. The applied voltage was linearly increased from 0 V to 3 V and the nonlinear current response of the Ta/IGZO/TaOx/Pt device to the applied voltage was measured. It was also observed that the device remained in its off state when the applied voltage was below ~2 V.

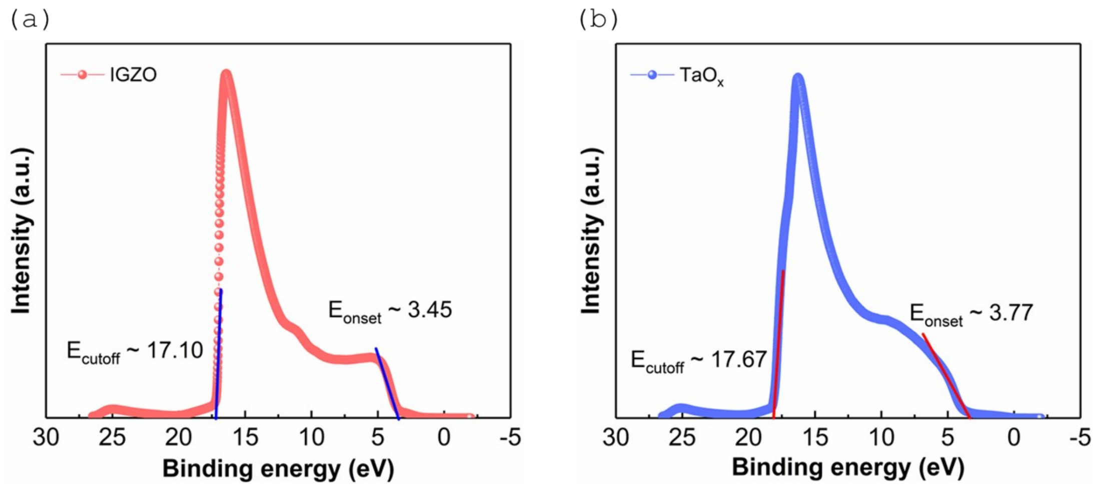

Figure S6. (a) UPS spectrum of TaO_x film. The E_{onset} and E_{cutoff} of TaO_x are evaluated to 3.77 eV and 17.67 eV, respectively. (b) UPS spectrum of IGZO film. The E_{onset} and E_{cutoff} of IGZO are evaluated to 3.45 eV and 17.10 eV, respectively.

The work function values are extracted from the UPS analyses using the expression given below.

$\phi(eV) = h\upsilon - E_{cutoff}$

$E_V\ (eV) = h\upsilon - (E_{cutoff} - E_{onset})$

Where, $\emptyset$ is the work function, $h\upsilon$ is the incident photon energy (21.2 eV), E_{cutoff} is the maximum energy which can excite the electrons, E_F is the Fermi energy in the spectrum (0 eV), E_V is the position of valance band, and E_{onset} is the Fermi edge position which denotes the onset of second electron emission. According to the UPS data of TaO_x and IGZO film shown in Figure S4, the obtained work function of TaO_x and IGZO is 3.53 eV and 4.10 eV, respectively.

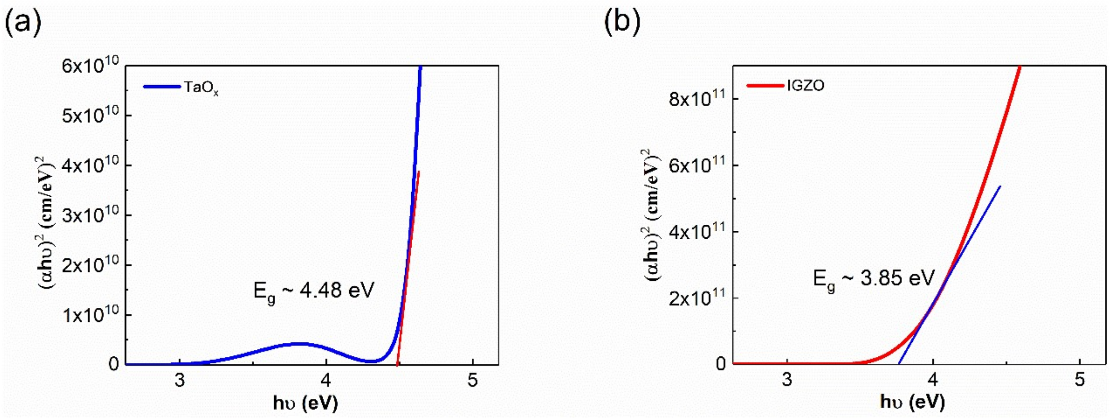

Figure S7. The Tauc's plot corresponding to $(\alpha h\upsilon)^2$ as a function of photon energy for the determination of the bandgap of TaO_x and IGZO, respectively.

Band gap values of TaO_x and IGZO are calculated from the Tauc plots obtained from UV-Vis transmission data, as shown in Fig. S5. The band gap value of TaO_x and IGZO are 4.48 eV and 3.85 eV, respectively.

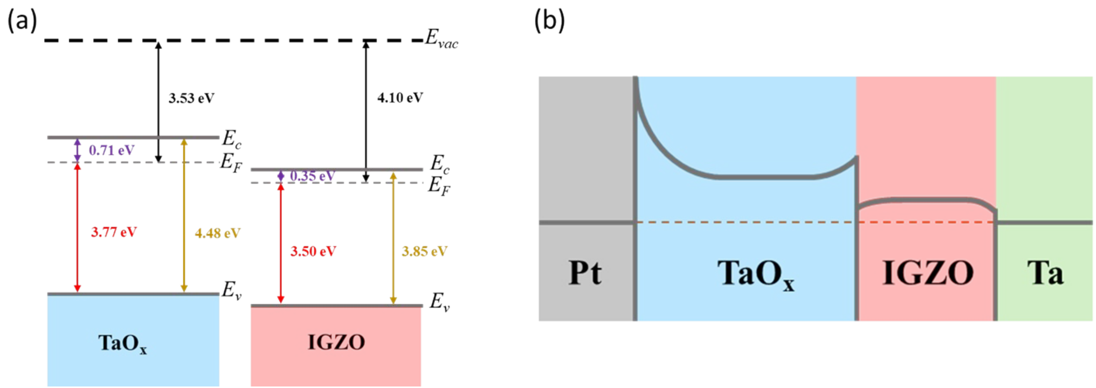

Figure S8. Energy band diagrams of TaO_x and IGZO (a) before contact and (b) after contact.

Combined with the work function values of the bottom electrode Pt (5.4 eV)[8] and the top electrode Ta (4 eV)[9] as well as the energy band diagrams of IGZO and TaO_x, the memristor band diagram was obtained by aligning all the fermi levels.

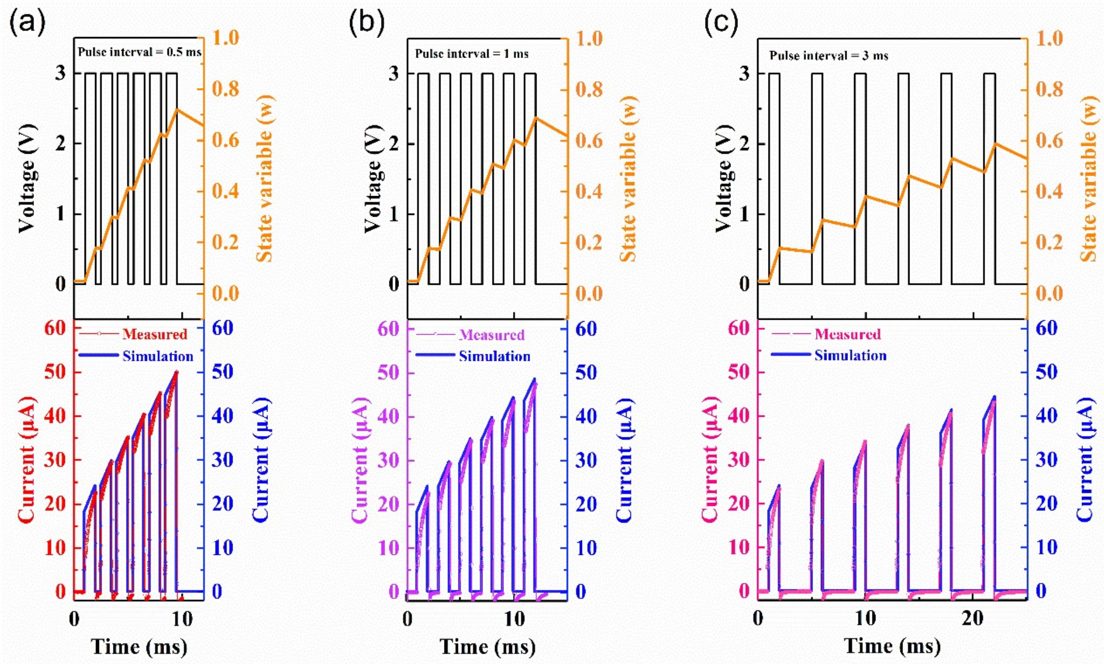

Figure S9. The top subfigures depict different voltage waveforms (black curves) and the dynamic change of the state variable (orange curves) under different pulse interval. In the bottom subfigures, the measured current responses are represented by the red curve for a pulse interval of 0.5 ms, the purple curve for a pulse interval of 1 ms, and the pink curve for a pulse interval of 3 ms. The simulated current response is illustrated by the blue curves.

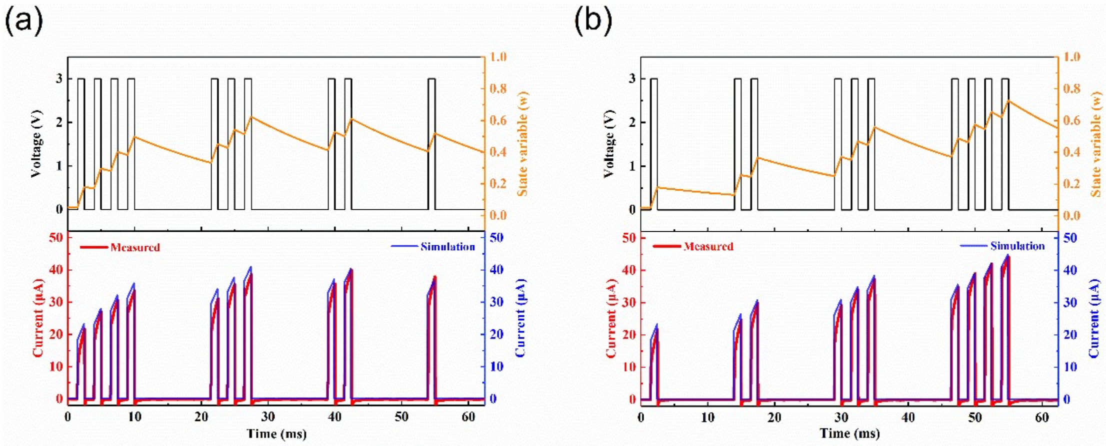

Figure S10. The top subfigures depict the voltage waveforms applied in each experiment, indicated by the black curves, along with the dynamic change of the state variable represented by the orange curves, under different pulse conditions. The bottom subfigures depict the measured current responses (red curves) and the fitted current responses (blue curves) corresponding to the applied voltage. To validate the accuracy of the memristor model, two voltage pulse waveforms were employed. (a) The decreasing number of applied pulses. (b) The increasing number of applied pulses.

Table S2. Parameters used in simulation for the IGZO/TaOx-based memristor device.

Parameter	Value
α	2.55e-5
β	$\frac{1}{3}$
γ	2.04e-6
δ	$\frac{4}{3}$
λ	1.08e-4
η	2.6
τ	25
w_0	0.05

References

1. J. K. Lee, O. Kwon, B. Jeon and S. Kim, *IEEE Trans. Electron Devices*, 2023, **70**, 5651-5656.
2. H. So, J.-K. Lee and S. Kim, *Appl. Surf. Sci.*, 2023, **625**, 157153.
3. D. Kim, J. Kim, S. Yun, J. Lee, E. Seo and S. Kim, *Nanoscale*, 2023, **15**, 8366-8376.
4. J. Park, T.-H. Kim, O. Kwon, M. Ismail, C. Mahata, Y. Kim, S. Kim and S. Kim, *Nano Energy*, 2022, **104**, 107886.
5. C. Du, F. Cai, M. A. Zidan, W. Ma, S. H. Lee and W. D. Lu, *Nat. Commun.*, 2017, **8**, 2204.
6. Y. Zhong, J. Tang, X. Li, B. Gao, H. Qian and H. Wu, *Nat. Commun.*, 2021, **12**, 408.
7. A. H. Jaafar, L. Shao, P. Dai, T. Zhang, Y. Han, R. Beanland, N. T. Kemp, P. N. Bartlett, A. L. Hector and R. Huang, *Nanoscale*, 2022, **14**, 17170-17181.
8. S. Trasatti, *Journal of Electroanalytical Chemistry and Interfacial Electrochemistry*, 1971, **33**, 351-378.
9. J. Hölzl and F. K. Schulte, in *Solid Surface Physics*, eds. J. Hölzl, F. K. Schulte and H. Wagner, Springer Berlin Heidelberg, Berlin, Heidelberg, 1979, DOI: 10.1007/BFb0048919, pp. 1-150.